ANL/TD/CP-97678

# DETERMINING PU-239 CONTENT BY RESONANCE TRANSMISSION ANALYSIS USING A FILTERED REACTOR BEAM

Raymond T. Klann
Argonne National Laboratory
9700 South Cass Avenue
Bldg. 362, Rm. B-133
Argonne, IL 60439
E-mail: klann@anl.gov



Manuscript submitted to the 6th NDA Waste Characterization Conference November 17-19, 1998
Salt Lake City, Utah

The submitted manuscript has been created by the University of Chicago as Operator of Argonne National Laboratory ("Argonne") under Contract No. W-31-109-ENG-38 with the U.S. Department of Energy. The U.S. Government retains for itself, and others acting on its behalf, a paid-up, nonexclusive, irrevocable worldwide license in said article to reproduce, prepare derivative works, distribute copies to the public, and perform publicly and display publicly, by or on behalf of the Government.

This work was supported by the U.S. Department of Energy, Energy Research Programs, under contract W-31-109-Eng-38.

# **DISCLAIMER**

This report was prepared as an account of work sponsored by an agency of the United States Government. Neither the United States Government nor any agency thereof, nor any of their employees, make any warranty, express or implied, or assumes any legal liability or responsibility for the accuracy, completeness, or usefulness of any information, apparatus, product, or process disclosed, or represents that its use would not infringe privately owned rights. Reference herein to any specific commercial product, process, or service by trade name, trademark, manufacturer, or otherwise does not necessarily constitute or imply its endorsement, recommendation, or favoring by the United States Government or any agency thereof. The views and opinions of authors expressed herein do not necessarily state or reflect those of the United States Government or any agency thereof.

# DISCLAIMER

Portions of this document may be illegible in electronic image products. Images are produced from the best available original document.

# DETERMINING PU-239 CONTENT BY RESONANCE TRANSMISSION ANALYSIS USING A FILTERED REACTOR BEAM

Raymond T. Klann
Argonne National Laboratory
9700 South Cass Avenue, Bldg. 362
Argonne, IL 60439
E-mail: klann@anl.gov

# **ABSTRACT**

A novel technique has been developed at Argonne National Laboratory to determine the <sup>239</sup>Pu content in EBR-II blanket elements using resonance transmission analysis (RTA) with a filtered reactor beam. The technique uses cadmium and gadolinium filters along with a <sup>239</sup>Pu fission chamber to isolate the 0.3 eV resonance in <sup>239</sup>Pu. In the energy range from 0.1 to 0.5 eV, the total microscopic cross-section of <sup>239</sup>Pu is significantly larger than the cross-sections of <sup>238</sup>U and <sup>235</sup>U. This large difference in cross-section allows small amounts of <sup>239</sup>Pu to be detected in uranium samples.

Tests using a direct beam from a 250 kW TRIGA reactor have been performed with stacks of depleted uranium and <sup>239</sup>Pu foils. Preliminary measurement results are in good agreement with the predicted results up to about two weight percent of <sup>239</sup>Pu in the sample. In addition, measured <sup>239</sup>Pu masses were in agreement with actual sample masses with uncertainties less than 3.8 percent.

### INTRODUCTION

The Experimental Breeder Reactor - II (EBR-II) is an unmoderated, heterogeneous, sodium-cooled, fast-breeder reactor operated by the Argonne National Laboratory (ANL) at the Idaho National Engineering and Environmental Laboratory (INEEL). The core consists of driver assemblies of uranium-zirconium metal or uranium-plutonium-zirconium metal surrounded by reflector assemblies of stainless steel and blanket assemblies of depleted uranium. These depleted uranium assemblies serve as an additional reflector and a breeder of <sup>239</sup>Pu.

EBR-II operation was terminated on September 30, 1994 after 30 years of operation. The shutdown plan for the reactor calls for the industrially and radiologically safe plant closure condition so that the reactor can be transferred to the Office of Environmental Management for

ultimate decontamination and decommissioning. The shutdown activity includes the treatment of the discharged driver and blanket assemblies in the Fuel Conditioning Facility (FCF).

A total of 353 depleted uranium blanket assemblies that were irradiated in EBR-II still exist today. Each blanket assembly consists of 19 elements as shown in Figure 1. Therefore, there are a total of 6707 blanket elements that must be processed in FCF. Currently, the plan is to process 25 blanket assemblies (475 elements) as part of the demonstration phase of the electrorefining treatment process. Because of criticality concerns and material control and accountability requirements in the processing of fissionable material in FCF, the fissionable material content of each assembly must be known with a reasonable degree of certainty prior to being transferred from EBR-II into FCF.

Over time, a small amount of the <sup>238</sup>U was bred into <sup>239</sup>Pu by neutron capture and subsequent beta decay through the following reaction:

$$^{238}U(n,\gamma)^{239}U \rightarrow ^{\beta^{-}} \rightarrow ^{239}Np \rightarrow ^{\beta^{-}} \rightarrow ^{239}Pu$$
.

To a much lesser extent, other heavy metals have also been bred into the blanket elements. The neutron capture reaction (n,γ) is highly dependent on neutron energy and exhibits strong resonances in the epithermal energy range. Resonances are isotope-dependent and based on the nuclear properties of the specific isotope. Estimates indicate that as much as 1000 grams of <sup>239</sup>Pu have been created in some blanket assemblies from an initial <sup>238</sup>U weight of about 48 kilograms. However, the estimated quantities of <sup>239</sup>Pu are highly suspect due to uncertainties in the flux characterization in the blanket region. Knowing that the estimates for plutonium buildup in blanket elements have large uncertainties and are most likely under predicted, the amount of <sup>239</sup>Pu in blanket elements should be measured. Methods of radiation-based non-destructive analysis were reviewed, <sup>1-7</sup> however, most of these have inherent problems or weaknesses for analyzing EBR-II blanket assemblies or elements. Therefore, a method was developed at ANL that uses a continuous, filtered neutron beam from a 250 kW TRIGA reactor to perform resonance transmission analysis. <sup>8</sup>

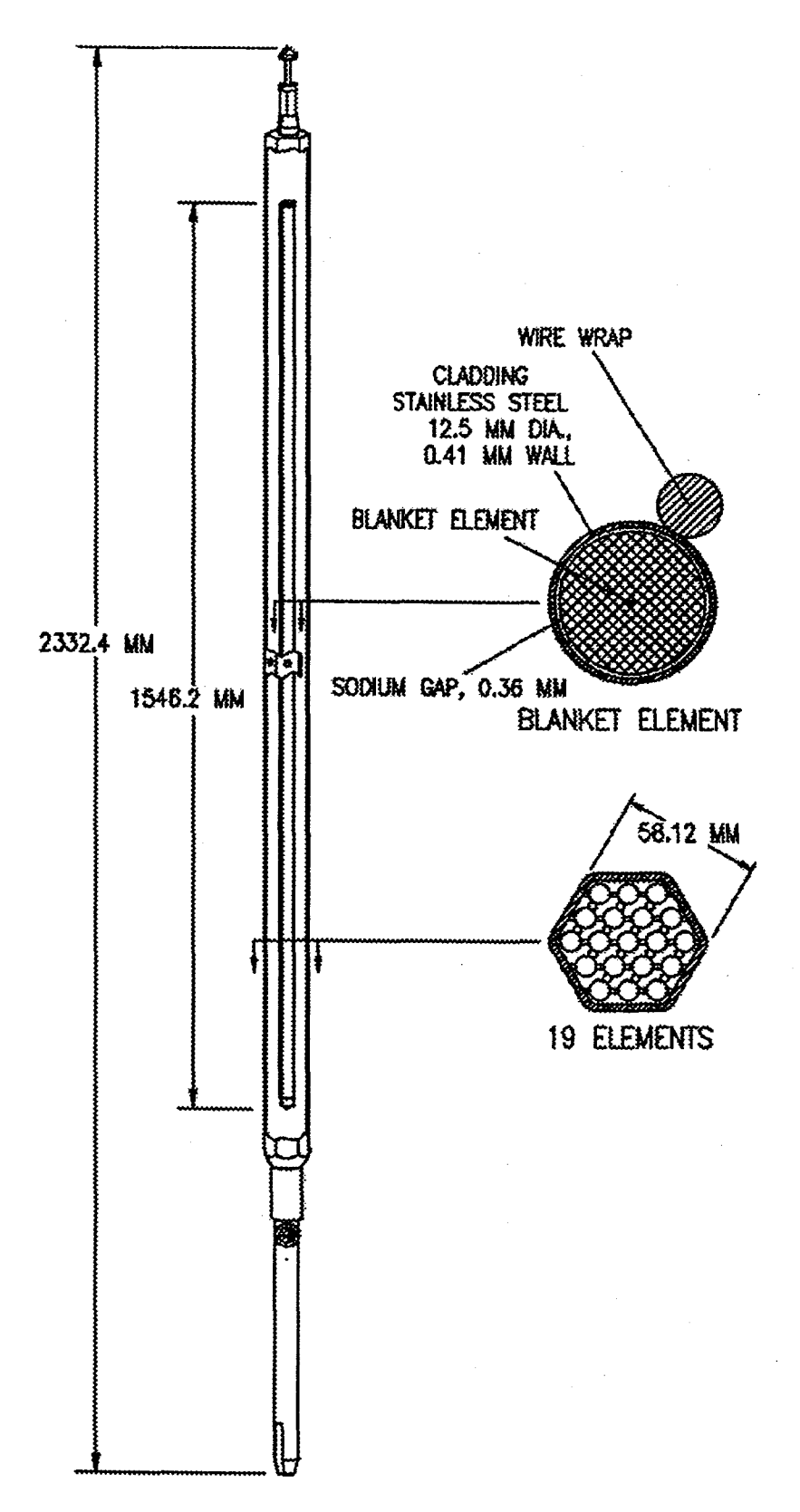


Figure 1: EBR-II Blanket Assembly

# MEASUREMENT TECHNIQUE

In order for an analysis method to be successful at determining small amounts of <sup>239</sup>Pu in large quantities of depleted uranium, there has to be a significant signal change for a small change in <sup>239</sup>Pu content. For the blanket elements, the only way that there can be a large signal change in transmission analysis is if the total neutron cross-section of <sup>239</sup>Pu in the sample is a large fraction of the total neutron cross-section of the sample. To accomplish this, a neutron energy or energy region must be chosen such that the microscopic total neutron cross-section of <sup>239</sup>Pu is much greater than the microscopic total neutron cross-section of the other isotopes in the sample, mainly <sup>238</sup>U and <sup>235</sup>U.

<sup>239</sup>Pu has a resonance at 0.3 eV of greater than 5000 barns as shown in Figure 2. Also shown in Figure 2 are the cross-sections for <sup>235</sup>U and <sup>238</sup>U. If this resonance can be reasonably isolated, then the amount of <sup>239</sup>Pu in a sample can be determined through the value of the transmission in this region. Cadmium and gadolinium filters along with a <sup>239</sup>Pu fission chamber are used as the means to isolate this resonance. The cadmium filter is used to define the upper bound of the energy region. The gadolinium filter is used to define the lower bound of the energy region. The <sup>239</sup>Pu fission chamber is used to enhance the response.

For a mono-energetic beam, the transmitted or uncollided flux through a sample of uniform thickness is defined as

$$\phi(x) = \phi(0) e^{-\Sigma_T x} ,$$

where  $\phi(0)$  is the flux incident on a sample of thickness x and  $\Sigma_T$  is the total macroscopic cross-section of the sample.  $\phi(x)$  is considered the transmitted flux, such that the transmission through the sample is defined as

$$T = \frac{\Phi(x)}{\Phi(0)} = e^{-\Sigma_T x}.$$

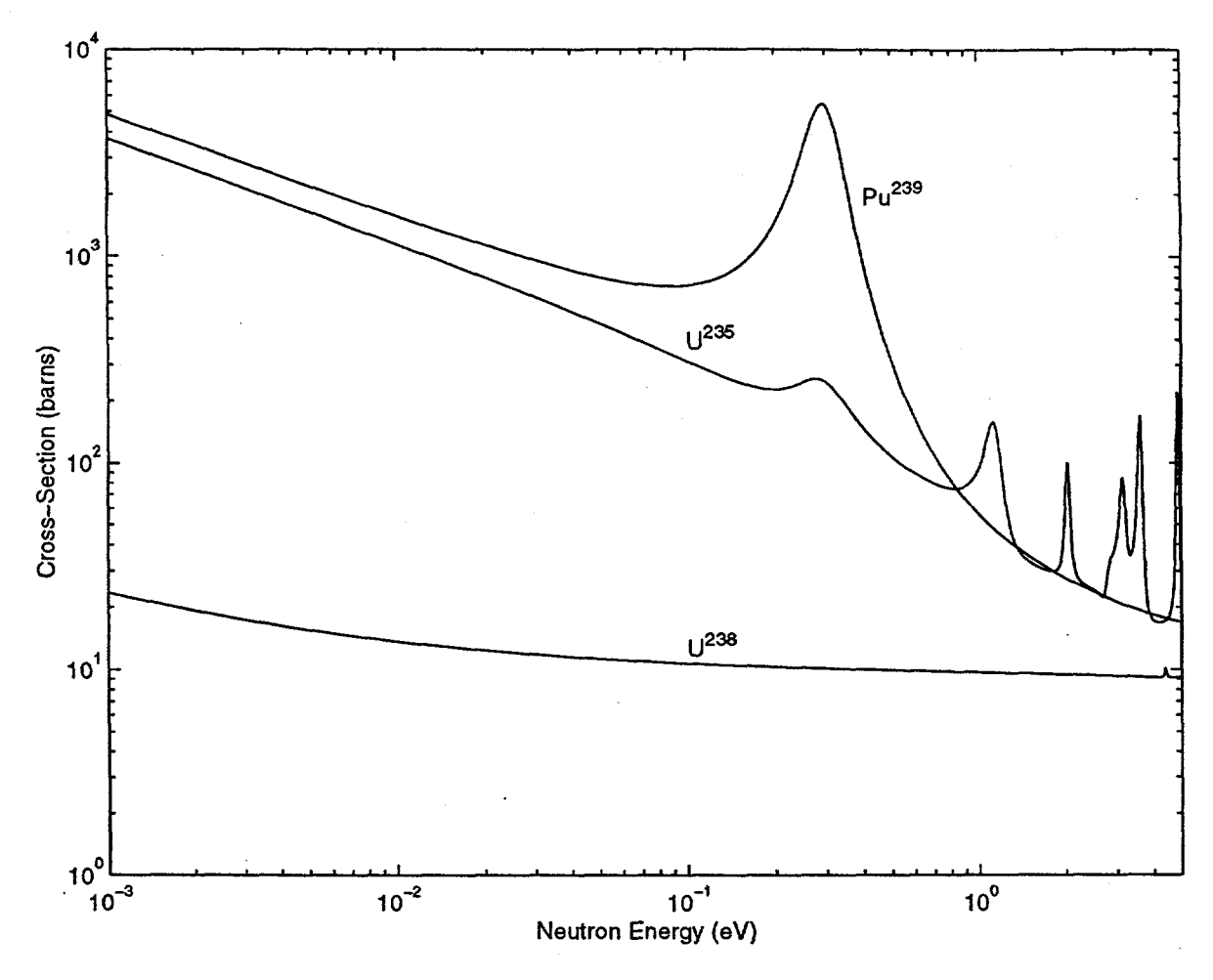


Figure 2: Total Cross-Sections of <sup>239</sup>Pu, <sup>238</sup>U, and <sup>235</sup>U

The transmission is a unitless term which has a value between zero (no transmission) and one (complete transmission), and is an exponential function of the macroscopic cross-section and the sample thickness. A further variable, the mass signal, is defined as

$$M = -\ln(T) = \Sigma_T x ,$$

which is a direct measure of the macroscopic cross-section since the sample thickness is assumed uniform.

Unfortunately, the neutron energy spectrum in a reactor beam is not mono-energetic. The spectrum in the east beam tube of the ANL Neutron Radiography (NRAD) Reactor has been

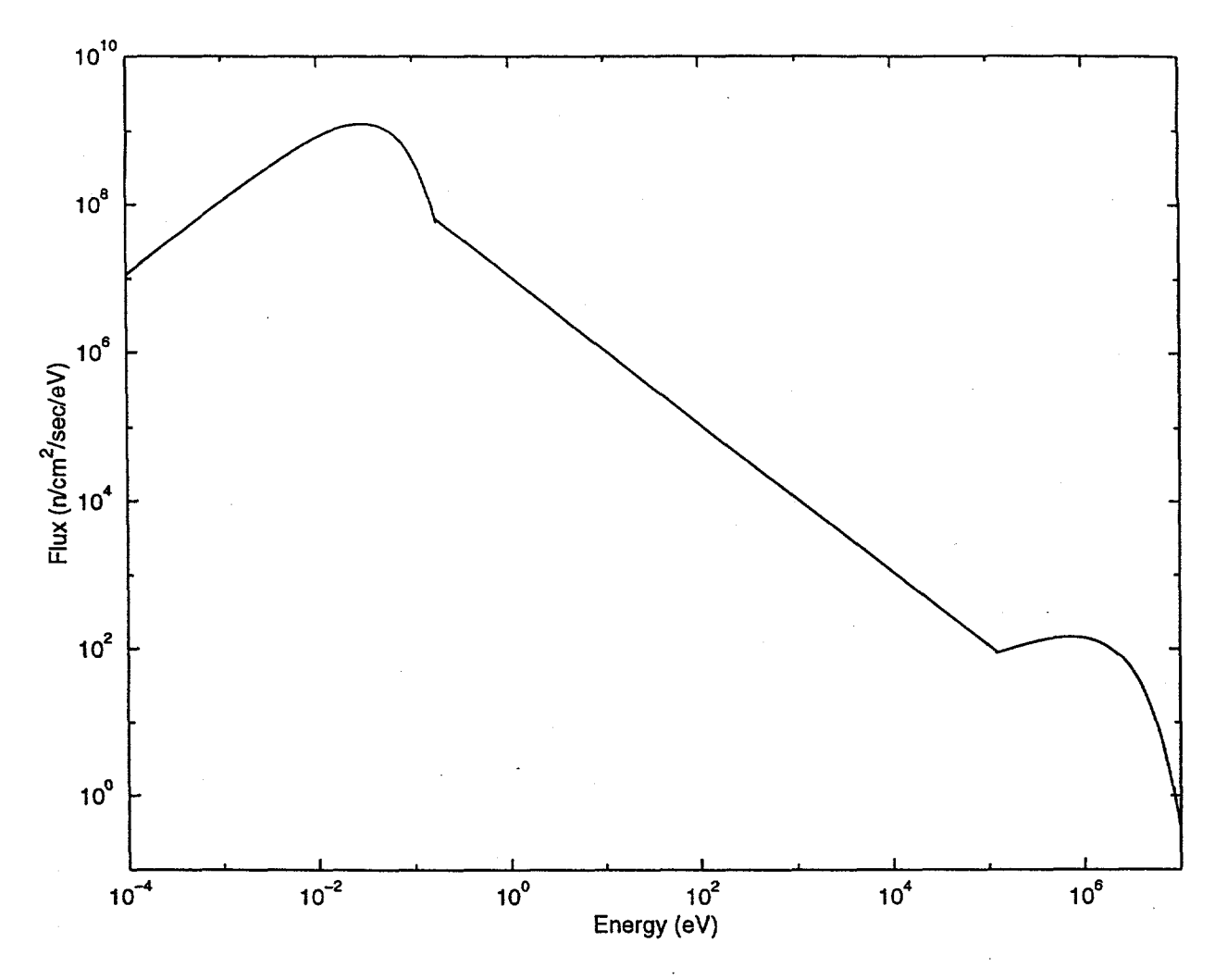


Figure 3: NRAD Spectrum

characterized by foil measurements<sup>9</sup> and is shown in Figure 3. A flux-averaged mass signal can be calculated and measured. However, the differences in cross-sections among isotopes is much smaller, and as such, the response to the change in the <sup>239</sup>Pu content is not significant. Therefore, a series of measurements using a gadolinium filter (0.01 cm thick) and a cadmium filter (0.1 cm thick) were used to isolate the energy region from 0.1 eV to 0.5 eV. In addition, a <sup>239</sup>Pu fission chamber was used to enhance the detector response as it is ideally suited for <sup>239</sup>Pu transmission measurements.<sup>8</sup>

Each mass signal determination is actually based on a combination of four individual measurements. The sample and the cadmium filter can be placed in and out of the beam

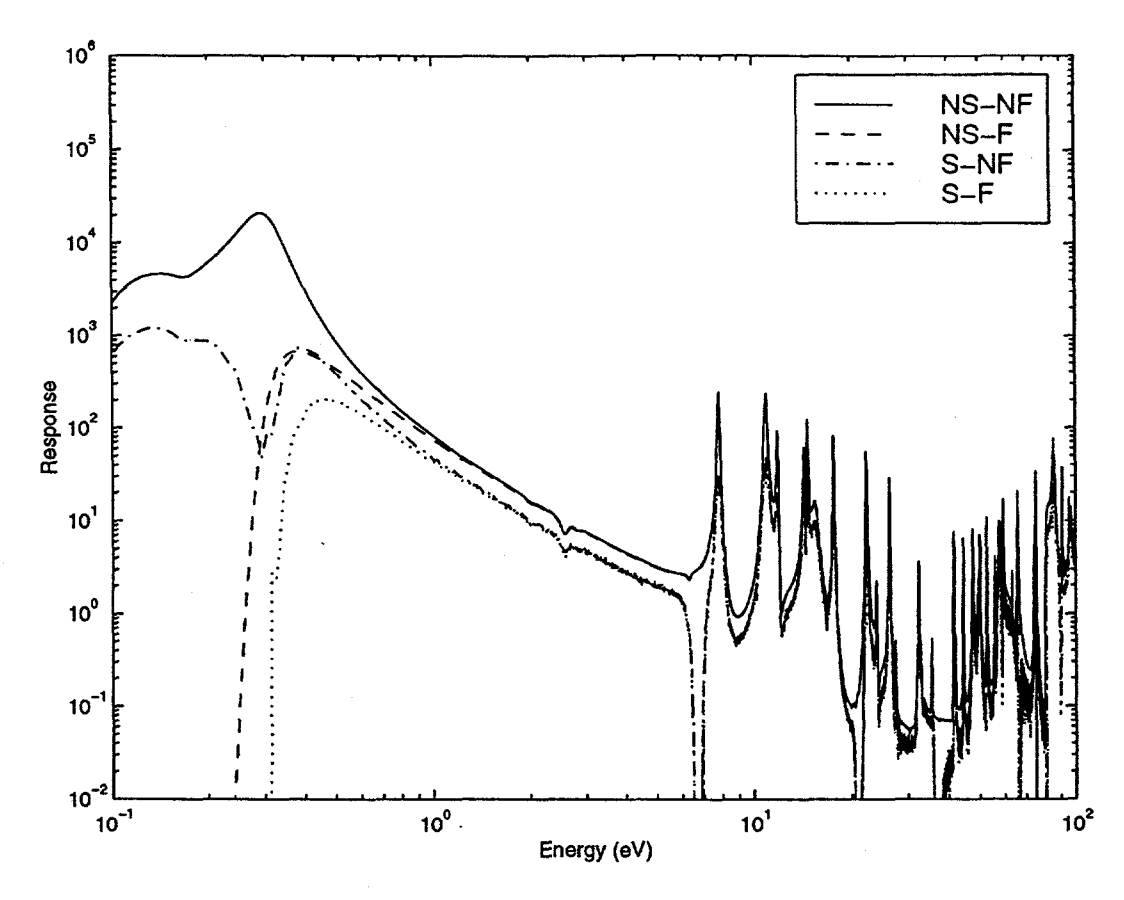


Figure 4: Spectral Detector Response of Different Filter/Sample Combinations

independently. The various sample-filter combinations result in four different measurements. Because the detector (a <sup>239</sup>Pu fission chamber) does not have a constant detector response over all neutron energies, the measured mass signal is not simply a flux-averaged mass signal. Instead it is a complicated combination of the flux spectrum, the energy dependent detector response, and the energy dependent cross-sections of the sample.

Figure 4 is a sample plot of the calculated detector response for the four configurations of sample and cadmium filter. The notation used in Figure 4 denotes the position of sample (S) and the cadmium filter (F). As an example, the plot noted as NS-F is for the case with no sample in the beam but the cadmium filter is in the beam. The gadolinium filter is in the beam for all cases. The figure is a log-log plot of the detector response versus the neutron energy. The y axis is shown as response. The response is the number of neutrons in that group from the total number of neutron histories. For the case shown, the number of neutron histories was  $10^7$  so these values

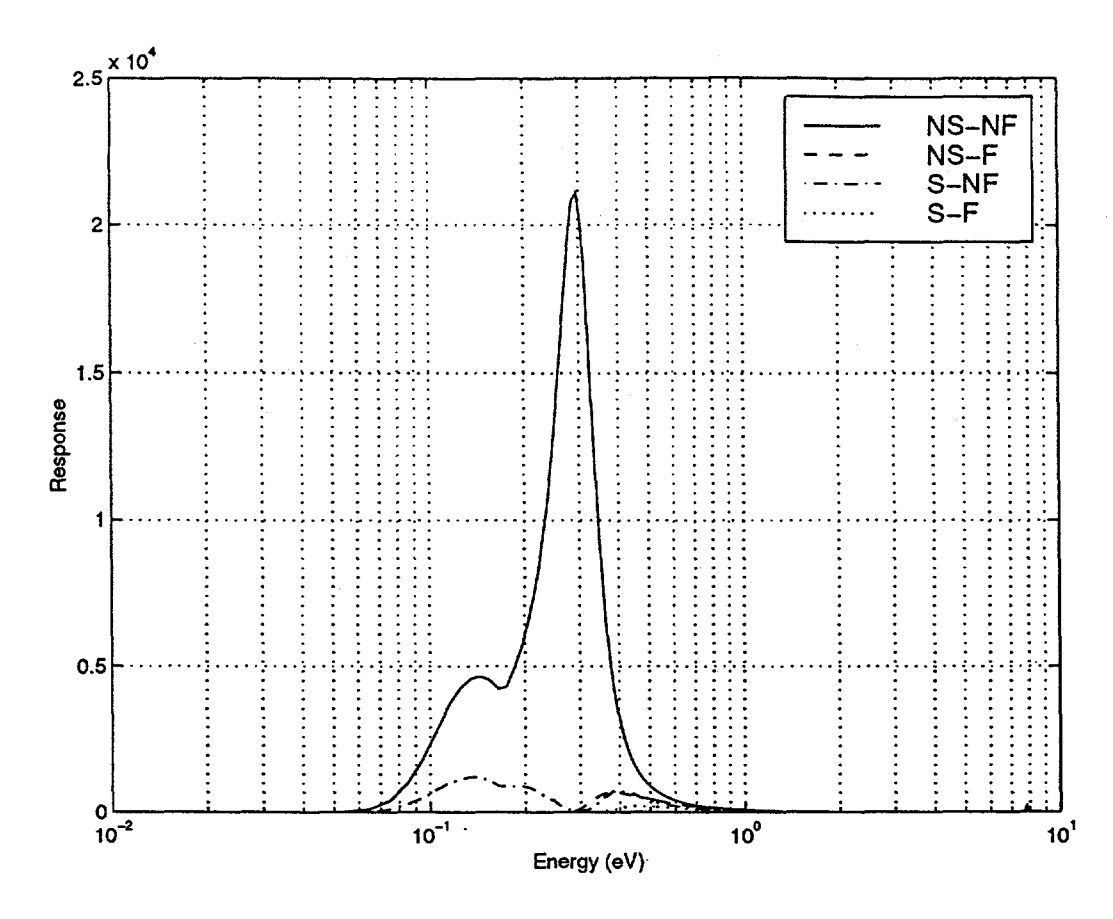


Figure 5: Spectral Detector Response (Semi-log Plot)

can be normalized by dividing by  $10^7$ . Although Figure 4 is only shown up to 100 eV, the resonance behavior of the filter and sample materials is readily apparent. It is also apparent that the 0.3 eV resonance in  $^{239}\text{Pu}$  clearly dominates the spectrum. The difference between the two curves, S-NF and NS-NF, is due to attenuation from the sample. The S-NF plot shows a deep depression in the spectrum around 0.3 eV of approximately two orders of magnitude. This depression is due to the effect that the  $^{239}\text{Pu}$  in the sample has on the attenuation. The S-F and NS-F cases also show a large drop off of greater than five orders of magnitude due to the cadmium filter. This supports the assumption that essentially everything below the cadmium cutoff energy is removed from the beam.

The benefit of the <sup>239</sup>Pu detector is shown in Figure 5. Figure 5 is a plot of the same information as in Figure 4 only plotted on a semi-log scale. This figure shows the dramatic peaking in the energy range of interest (0.1 eV to 0.5 eV) and demonstrates that this filtered beam transmission

method effectively isolates the 0.3 eV resonance in <sup>239</sup>Pu. Also shown in Figure 5 is the effect of the gadolinium filter. The gadolinium filter significantly reduces the neutrons below the resonance (less than 0.1 eV) while still allowing the neutrons with higher energies to pass through it with little effect. There is a small bump or second peak in the response spectrum at about 0.15 eV. This peak is due to the gadolinium filter not totally removing the neutrons from an increased neutron flux. As shown in Figure 3, the flux is increasing in this energy range as the neutron energy decreases.

During each measurement, there is also a fission chamber in the ERS cell monitoring the flux level of the reactor. The measurement from the flux monitor was used to normalize each measurement. Background measurements were performed prior to the experiment and were consistent regardless of the position of the sample and filter. The mass signal is computed from the measurements as follows:

$$M_{M} = \frac{\left(\frac{C}{M}\right)_{S-NF} - \left(\frac{C}{M}\right)_{S-F}}{\left(\frac{C}{M}\right)_{NS-NF} - \left(\frac{C}{M}\right)_{NS-F}},$$

where  $M_M$  represents the mass signal computed from the measurements, C represents the count rate from the detector in the beam, and M represents the count rate of the flux monitor. The subscripts on the C/M ratios indicate the position of the sample and the filter during the measurement, as described previously. The background count rates are not included in the above equation. It was demonstrated that they were correlated for the four measurements are were reduced from the mass signal equation. The standard deviation of the mass signal values was calculated from the error propagation formula.

### **EXPERIMENTAL SET-UP**

The equipment to perform these measurements consists of three major systems in addition to the reactor facility - the beam collimator, the experiment table and the detection equipment. Figure 6 shows a schematic of the layout of the experimental equipment. The collimator and experiment table are both located in the ERS Cell of the NRAD Reactor Facility. The detectors are also located within the cell, however, the associated electronics are located external to the cell. Cabling between the electronics and the detectors are located in conduit that penetrates the shielding walls of the ERS Cell.

The NRAD Reactor was installed in the Hot Fuel Examination Facility (HFEF) at Argonne National Laboratory in 1977. The reactor is a 250 kW steady-state heterogeneous water-moderated TRIGA type reactor<sup>10-12</sup>. The ERS cell and radiography station were designed to provide a beam of neutrons so that reactor fuel elements and structural components located in the main cell of HFEF could be radiographed without leaving the cell. The east beam tube looks directly at the core and offers a harder spectrum than other reactor facilities that have tangential beams. The spectrum of the beam was shown in Figure 3.

The east beam tube was designed for radiography and, as such, has a very large beam area within the ERS Cell. The beam area is defined by a boron nitride aperture disk and a through-the-wall collimator. The beam area is much larger than the intended samples and had to be reduced and collimated for the experiment. A collimator was built using 34 sheets of borated polyethylene. The sheets are 61 centimeters by 91 centimeters wide and 2.5 centimeters thick. The boron content of the sheets is 15% by weight. Different diameter holes were drilled in each sheet so that when stacked together the hole through all of the sheets would resemble a cone. The hole at the front of the collimator had a diameter of 2.858 centimeters and the hole at the back of the collimator had a diameter of 0.635 centimeters. The conical hole is a convergent collimator and was sized to align with the hole in the boron nitride aperture disk.

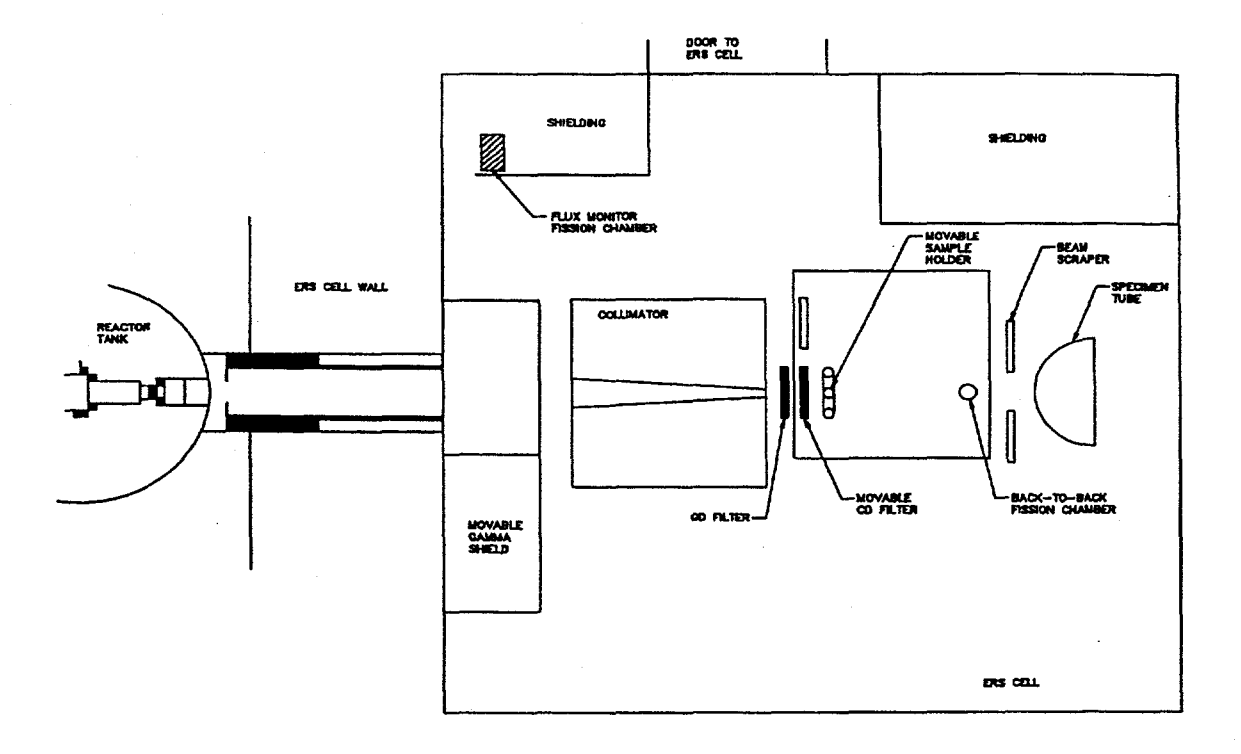


Figure 6: Schematic Layout of Experiment

With the collimator in place, the beam had a divergent angle of 0.85°. This angle with the positioning of the sample created a beam diameter of 1.02 centimeters at the sample. The beam diameter at the detector was 2.87 centimeters. The smallest diameter of the foils was 1.08 centimeters. This meant that the entire beam passed through the sample. The detector area was smaller than the beam area at the detector so every neutron interacting with the detector had to pass through the sample (except background neutrons). This is ideal for a transmission experiment. What should be avoided is beam neutrons that can reach the detector without passing through the sample. If the neutrons causing reactions in the detector did not pass through the sample then the mass signal will not vary as much due to compositional changes in the sample because there will always be a large part of the signal which is unaffected by the sample. This is the same reason that the background rate should be reduced to as low as reasonably achievable. With the geometry of the collimator and placement of the sample and detector shown, the entire beam passed through the sample and a portion of this beam interacted with the detector.

The experiment table was a simple construction of aluminum angle, sheet, and bars to support the experimental equipment. The experimental equipment mounted on the table consisted of two linear actuators and the detector mounting. The actuators were used to independently position a cadmium filter (0.1 cm thick) and a sample holder in and out of the beam. The detector mounting was used to fix the position of a <sup>239</sup>Pu fission chamber in the beam.

The samples used for the measurements consisted of a stack of 1.27 cm diameter foils of <sup>239</sup>Pu, <sup>235</sup>U, <sup>238</sup>U, and stainless steel. The sample holder was composed of stainless steel and the SS disks were used to maintain the reference measurements consistent. The other foils were used to mock-up the thickness of a blanket element and to vary the plutonium content in the sample.

#### EXPERIMENTAL RESULTS

Measurements were performed to determine the mass signal value as a function of <sup>239</sup>Pu content in the sample. The number of foils was determined by setting the theoretical density foil thickness equal to the thickest portion of a blanket element. <sup>238</sup>U foils were then removed and <sup>239</sup>Pu foils were added to obtain different <sup>239</sup>Pu contents in the sample. This replacement simulated the conversion of <sup>238</sup>U to <sup>239</sup>Pu in a blanket element by maintaining the sample mass as close to the nominal value as possible.

The results of the measurements are shown in Table 1. Figure 7 shows the data plotted vs. the weight percent of <sup>239</sup>Pu. Also shown is a curve fit of the calculated values adjusted with a constant bias. As observed from Figure 7, the measured values are in good agreement with the calculated values with a constant bias up to about two weight percent of <sup>239</sup>Pu. The values start to deviate from expected as the <sup>239</sup>Pu content is increased. The bias is constant for the measurements performed and represents isotopes in the <sup>238</sup>U foils not accounted for in the calculations, most notably hydrogen in the glue used to attach thin aluminum foils on the front and back of each foil. Using a microscopic total cross-section of approximately 20 barns for hydrogen, the bias from the measurements of 0.1525, and a sample thickness of 1.1 cm results in

Table 1: Results of Measurements					
<sup>239</sup> Pu Content		Standard	Mass	Standard	
(wt%)	Transmission	Deviation	Signal	Deviation	
0	0.480	0.0024	0.733	0.0050	
0	0.479	0.0021	0.736	0.0044	
0.073	0.427	0.0020	0.851	0.0047	
0.179	0.362	0.0018	1.015	0.0051	
0.657	0.192	0.0016	1.648	0.0084	
0.657	0.199	0.0014	1.615	0.0071	
0.789	0.173	0.0014	1.754	0.0078	
0.918	0.150	0.0013	1.895	0.0085	
0.990	0.142	0.0010	1.955	0.0071	
1.370	0.103	0.0014	2.269	0.0132	
1.370	0.100	0.0011	2.306	0.0115	
1.606	0.086	0.0011	2.453	0.0128	
2.055	0.071	0.0011	2.641	0.0147	
2.647	0.050	0.0012	3.001	0.0239	
3,177	0.044	0.0012	3.114	0.0260	

a density of 0.012 g/cm<sup>3</sup> for the hydrogen in the sample. This is 0.063 weight percent of hydrogen in the sample, which translates into 0.19 mg of hydrogen in a depleted uranium foil that weighs 300 mg.

The transmission is an exponential function of the mass signal. Now assume that there is a limit to the mass signal such that the transmission is so small that it can be assumed to be zero. This value of the mass signal is the saturation point. No further attenuation of the beam occurs since the transmission is zero. The mass signal of a sample is a function of the microscopic cross-section multiplied by the atom density and the sample thickness. This means that as the atom density of <sup>239</sup>Pu increases, saturation is attained at energies that correspond to the highest cross-sections first. Continually increasing the <sup>239</sup>Pu content in the sample then causes saturation to occur at continually lower cross-section values. As the <sup>239</sup>Pu content increases, saturation occurs at the peak of the resonance which causes the sample to become "black" at this energy such that there is no measurable transmission. As the <sup>239</sup>Pu content continues to be increased, saturation starts to occur at energies adjacent to the peak of the resonance. Eventually, the entire energy range of interest is saturated and the mass signal becomes constant. In theory, the mass signal

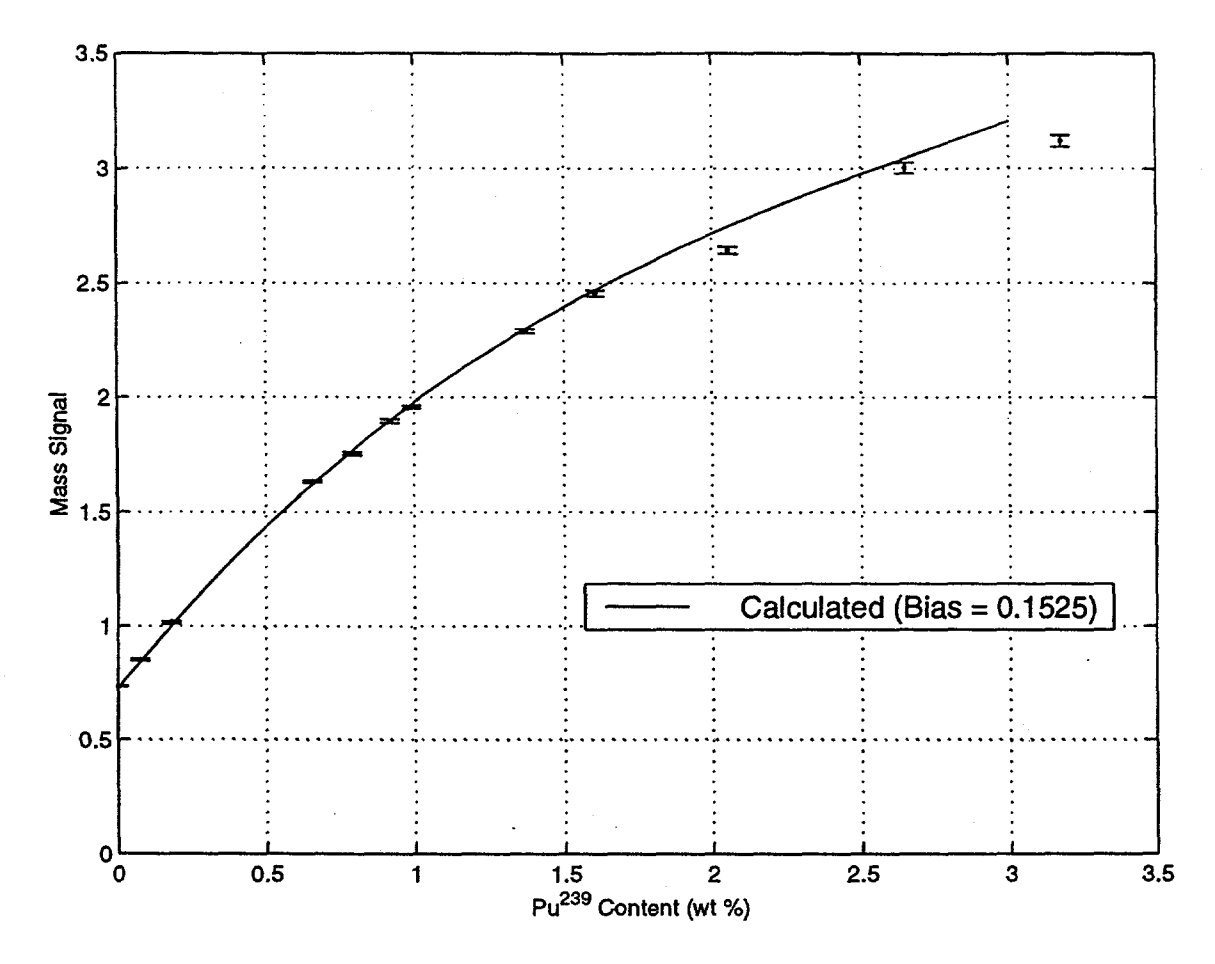


Figure 7: Mass Signal as a Function of <sup>239</sup>Pu Content

would approach an asymptote at this value. In practice, a point is reached at which the measured mass signal plus the standard deviation of the mass signal reaches the asymptote. This describes a limit to the amount of <sup>239</sup>Pu that can be determined in a sample, however, it does not explain the deviation between the predicted mass signal and the measured mass signal at <sup>239</sup>Pu contents above two weight percent.

The difference between the calculated values and measured values could be due to a discrepancy in the cross-sections of <sup>239</sup>Pu in the valleys of the resonances. It is known that the evaluated functions used to describe the cross-sections between the resonances tend to over predict the cross-sections in these regions. This can be observed by reviewing the measured cross-section data points compared to the evaluated data for <sup>239</sup>Pu. <sup>13</sup> If a larger cross-section value is used to compute the mass signal then the mass signal will also be over predicted. This trend becomes

apparent at <sup>239</sup>Pu contents greater than two weight percent. This is observed in Figure 7 as the discrepancy between measured and predicted mass signals becomes larger. Above two weight percent of <sup>239</sup>Pu, saturation has occurred in the energy range of the 0.3 eV resonance. Therefore, the transmission is primarily due to neutrons at energies corresponding to lower cross-section values. Since the actual cross-sections are slightly lower than the evaluated cross-section data used for the calculations, the measured mass signal is lower than the calculated mass signal. As the <sup>239</sup>Pu content is increased, more neutrons with energies which correspond to lower cross-section values contribute to the transmission. This causes the measured mass signal to further deviate from the calculated mass signal. To use this method above two weight percent <sup>239</sup>Pu, a calibration function is necessary to accurately predict the <sup>239</sup>Pu content. This calibration function should be generated from measurements on actual samples, since it has been observed that the calculational estimates over predict the <sup>239</sup>Pu content in the samples.

After it was demonstrated that there is a significant change in mass signal with <sup>239</sup>Pu content and that this filtered method can accurately predict the mass signal, it was desirable to determine the error in such a measurement. Two samples were prepared from foils with known quantities of <sup>239</sup>Pu. The mass signal was determined from measurement, and this value was used to determine the <sup>239</sup>Pu content of the sample based on a calibration curve. The calibration curve was established based on the calculated values and previously measured values. A constant bias was computed from the previously measured data compared to the calculations. The data were fit with a fifth-order polynomial function described by

$$P = Am^5 + Bm^4 + Cm^3 + Dm^2 + Em + F + b ,$$

where P is the <sup>239</sup>Pu content in weight percent; m is the mass signal; A, B, C, D, E, and F are constants from the fitting routine; and b is the bias. The <sup>239</sup>Pu content was then predicted from the measurement of the mass signal. Also, based on this function the error in the <sup>239</sup>Pu content was determined from the mass signal and the error on the mass signal. The standard deviation on the <sup>239</sup>Pu content is

Table 2: Predicted <sup>239</sup> Pu Content for Test Samples					
Actual <sup>239</sup> Pu Content (wt%)	1.023	2.205			
Adjusted Mass Signal from Measurement	1.969	2.807			
Uncertainty in Mass Signal	0.011	0.02			
<sup>239</sup> Pu Content from Measurement (wt%)	1.011	2.301			
Uncertainty in <sup>239</sup> Pu Content (wt%)	0.024	0.084			
Difference between Measured and Actual (%)	1.17	4.35			
<sup>239</sup> Pu Mass from Measurement	266.9 ±6.4 mg	608.6 ±22.3 mg			

$$\sigma_P^2 = (5Am^4 + 4Bm^3 + 3Cm^2 + 2Dm + E)^2 \sigma_m^2 + m^{10} \sigma_A^2 +$$

$$m^8 \sigma_B^2 + m^6 \sigma_C^2 + m^4 \sigma_D^2 + m^2 \sigma_E^2 + \sigma_F^2 + \sigma_b^2 ,$$

where  $\sigma$  is the standard deviation of each parameter and the other terms are as defined previously.

Two measurements were performed on test samples. The results are shown in Table 2. The actual <sup>239</sup>Pu content in each sample was determined from the known masses of the foils used to create the samples. The mass signal was then determined from the measurements and adjusted for the hydrogen content in the foils. The <sup>239</sup>Pu content in the sample was then determined based on the measured mass signal. The uncertainties were computed as previously discussed.

The difference between the measured <sup>239</sup>Pu content and the actual <sup>239</sup>Pu content is 1.2 percent for the first sample shown in Table 2. The uncertainty in the <sup>239</sup>Pu content is approximately 2.4 percent, so the measured quantity is in agreement with the actual quantity of <sup>239</sup>Pu in the sample. The difference between the measured <sup>239</sup>Pu content and the actual <sup>239</sup>Pu content is 4.4 percent for the second sample shown in Table 2. The uncertainty in the <sup>239</sup>Pu content is approximately 3.8 percent. The measured <sup>239</sup>Pu content is within two standard deviations of the actual <sup>239</sup>Pu content in the sample, which indicates a reasonable agreement between the two values. These two cases demonstrate that this approach can be used to accurately measure the <sup>239</sup>Pu content in depleted uranium samples.

## SUMMARY AND CONCLUSIONS

This report describes an experiment performed at ANL using the east beam of the NRAD reactor facility. Resonance transmission analysis using the time-of-flight (TOF) technique has been demonstrated by other researchers to yield accurate results of isotopic compositions in small samples and in waste drums. The TOF technique requires a high intensity pulsed neutron source which was not available at ANL. Therefore, the goal of the experiment was to demonstrate that resonance transmission analysis using a filtered neutron beam could be used to determine the <sup>239</sup>Pu content in a depleted uranium sample. The depleted uranium samples were identical in thickness to the diameter of EBR-II blanket elements. By using comparative samples, the usefulness of this approach for determining the <sup>239</sup>Pu content in EBR-II blanket elements was assessed.

It was demonstrated that the mass signal could be obtained from a simple equation relating the flux normalized count rate from four measurements with different sample/filter combinations. It was also demonstrated that the 0.3 eV resonance in <sup>239</sup>Pu was isolated such that the response of the measurement technique, the mass signal value, was based on the total cross-section of the sample over a small energy region around 0.3 eV.

By selecting this small energy region, the total cross-section of <sup>239</sup>Pu was significantly greater than the cross-sections of <sup>238</sup>U and <sup>235</sup>U as shown in Figure 2. Since the mass signal is the sum of the total macroscopic cross-sections of the constituent isotopes multiplied by the sample thickness, small changes in the <sup>239</sup>Pu content result in large changes in the mass signal. This was demonstrated for sample compositions up to three weight percent <sup>239</sup>Pu for a sample with a thickness equivalent to a blanket element.

The measurement results indicated good agreement with the calculational values corrected by a constant bias. The bias was found to be from additional material in the depleted uranium foils that was not accounted for in the analysis. It was postulated that the effect was due to hydrogen in the glue used to apply aluminum foils to the front and back of the foils. The hydrogen content

in each foil was determined to be approximately 0.19 mg, which is approximately 0.06 weight percent.

An apparent slight deviation between the measured and calculated values of <sup>239</sup>Pu in the sample was observed above two weight percent of <sup>239</sup>Pu. It was postulated that this deviation is due to a discrepancy in the cross-sections of <sup>239</sup>Pu in the valley of the resonances highlighted by saturation occurring at the higher cross-sections of the resonances. Above two weight percent, the atom density of <sup>239</sup>Pu becomes large enough that the transmission at energies with large cross-sections becomes essentially zero. At this point, the sample becomes a "black body" or a true absorber at these energies. As the <sup>239</sup>Pu content increases, the sample becomes black at more and more neutron energies. When the sample becomes black at all neutron energies corresponding to the <sup>239</sup>Pu resonances, the measured mass signal is based primarily on the lower cross-sections. It is known that the cross-sections in the valleys of the resonances are over predicted, and therefore, the calculated mass signal is also over predicted. This deviation does not indicate the limit of the measurement system as it can be accounted for by generating a calibration curve from measured data.

There is a practical limit for the technique based on the counting statistics. The transmission is an exponential function. As the <sup>239</sup>Pu content is increased, the transmission becomes smaller and smaller. Based on the statistics, at some <sup>239</sup>Pu content the uncertainty in the transmission is larger than the transmission. This translates into an upper bound on the mass signal and a limit of detectability on the <sup>239</sup>Pu content. At this level of <sup>239</sup>Pu content, the mass signal cannot be distinguished within statistics from the limit on the mass signal, and the <sup>239</sup>Pu content would be greater than the limit of detectability.

Once the calculated predictions of mass signal as a function of <sup>239</sup>Pu content were verified, several test samples were measured to determine the <sup>239</sup>Pu content from the measured mass signal values. These tests were used to demonstrate the method in which the <sup>239</sup>Pu content would be determined and to show that the measured <sup>239</sup>Pu content agreed well with the known quantities. These tests also demonstrated the error expected from such a measurement. The

Table 3: Summary of Measurements on Unknown Samples				
	Sample 1	Sample 2		
Sample Mass (g)	26.416	26.445		
<sup>239</sup> Pu Composition (wt%)	1.023	2.205		
<sup>239</sup> Pu Mass (mg)	270.1	583.1		
Measured <sup>239</sup> Pu Mass (mg)	266.9 ±6.4	608.6 ±22.3		

results of the two measurements are summarized in Table 3. The predicted <sup>239</sup>Pu masses shown in Table 3 are in good agreement with the actual <sup>239</sup>Pu masses of the two samples.

Resonance transmission analysis using a filtered reactor beam has been shown to be a viable method for determining <sup>239</sup>Pu content in depleted uranium samples. This method could be expanded, through the use of different filter materials, to assay other isotopes of interest, most notably <sup>235</sup>U or <sup>240</sup>Pu. With a movable gadolinium filter, a series of measurements could be performed to obtain a mass signal value for energies less than 0.1 eV, in addition to the energy range from 0.1 eV to 0.5 eV. With two different mass signals, the <sup>235</sup>U content could potentially be determined by comparing the mass signal ratio between the two energy regions. By the use of an indium filter, which has a resonance at 1.4 eV, in conjunction with a cadmium filter, the energy region from 0.5 eV to 1.4 eV could be isolated. The 1 eV resonance of <sup>240</sup>Pu might then be used to determine the <sup>240</sup>Pu content. These are just a few of the possibilities where resonance transmission analysis with filtered neutron beams might be applied.

# **ACKNOWLEDGMENTS**

This work was supported by the U.S. Department of Energy, Energy Research Programs, under contract W-31-109-Eng-38.

#### REFERENCES

- 1. D. Reilly, et aliene, <u>Passive Nondestructive Assay of Nuclear Materials</u>, U.S. Government Printing Office, 1991.
- 2. H.O. Menlove, et aliene, "The Design and Calibration of the Spent-Fuel Neutron

NOV-09-98 15:43

+6302521885

- Coincidence Counter for Underwater Applications," Los Alamos National Laboratory Report, Report No. LA-12769-MS, May 1994.
- 3. H.O. Menlove, "Description and Operation Manual for the Active Well Coincidence Counter," Los Alamos National Laboratory Report, Report No. LA-7823-M, May 1979.
- 4. P.M. Rinard, "Shuffler Instruments for the Nondestructive Assay of Fissile Materials," Los Alamos National Laboratory Report, Report No. LA-12105, May 1991.
- 5. S.E. Aumeier and J.H. Forsmann, "Kalman Filter Analysis of Delayed Neutron Non-Destructive Assay Measurements," Proceedings of the Third Topical Meeting on DOE Spent Nuclar Fuel and Fissile Material Management, Charleston, South Carolina, September 8-11, 1998.
- 6. R.A. Schrack, "Uranium-235 Measurement in Waste Material by Resonance Neutron Radiography," Nuclear Technology, November 1984, vol. 67, pages 326-332.
- 7. C.D. Bowman, et aliene, "Neutron Resonance Transmission Analysis of Reactor Spent Fuel Assemblies," Proceedings of the First World Conference on Neutron Radiography, D. Reidel Publishing Company, 1983, pages 503-511.
- 8. R.T. Klann and W.P. Poenitz, "Non-Destructive Assay of EBR-II Blanket Elements Using Resonance Transmission Analysis," Argonne National Laboratory Report, Report No. ANL/NDM-146, August, 1998.
- 9. G.R. Imel and T. Urbatsch, "Beam Characterization at the Neutron Radiography Facility (NRAD)," Proceedings of the Fourth World Conference on Neutron Radiography, Gordon and Breach Science Publishers, 1994, pages 673-681.
- 10. HFEF/N Neutron Radiography Facility Reactor Safety Analysis Report, Argonne National Laboratory Document No. W0170-0015-SA-00, August 1977.
- 11. HFEF/N Neutron Radiography Facility System Design Description, Argonne National Laboratory Document No. W0170-0004-SA-03, June 1978.
- 12. HFEF/N Neutron Radiography Facility North Radiography Station System Design Description, Argonne National Laboratory Document No. W0170-4002-ES-05, March 1982.
- 13. P.F. Rose, "ENDF-201, ENDF/B-VI Summary Documentation," Brookhaven National Laboratory Report, Report No. BNL-NCS-1741, 4th edition, October 1991.